STEM CELLS AND DEVELOPMENT
Volume 00, Number 00, 2016

DOI: 10.1089/scd.2016.0054

ORIGINAL RESEARCH REPORT

The CS Sulfation Motifs 4C3, 7D4, 3B3[–]; and Perlecan Identify Stem Cell Populations and Their Niches, Activated Progenitor Cells and Transitional Areas of Tissue Development in the Fetal Human Elbow

Anthony J. Hayes,[1] Clare E. Hughes,[2] Susan M. Smith,[3] Bruce Caterson,[2] Christopher B. Little,[3,4] and James Melrose[3–5]

We compared the immunohistochemical distribution of (1) the novel chondroitin sulfate (CS) sulfation motifs 7D4, 4C3, and 3B3[–], (2) native heparan sulfate (HS) and Δ-HS ''stubs'' generated by heparitinase III digestion and (3) the HS-proteoglycan (PG), perlecan, in the fetal human elbow joint. Putative stem cell populations associated with hair bulbs, humeral perichondrium, humeral and ulnar rudiment stromal/perivascular tissues expressed the CS motifs 4C3, 7D4, and 3B3[–] along with perlecan in close association but not colocalized. Chondrocytes in the presumptive articular cartilage of the fetal elbow expressed the 4C3 and 7D4 CS sulfation motifs consistent with earlier studies on the expression of these motifs in knee cartilage following joint cavitation. This study also indicated that hair bulbs, skin, perichondrium, and rudiment stroma were all perlecan-rich progenitor cell niches that contributed to the organization and development of the human fetal elbow joint and associated connective tissues. One of the difficulties in determining the precise role of stem cells in tissue development and repair processes is their short engraftment period and the lack of specific markers, which differentiate the activated stem cell lineages from the resident cells. The CS sulfation motifs 7D4, 4C3, and 3B3[–] decorate cell surface PGs on activated stem/progenitor cells and thus can be used to identify these cells in transitional areas of tissue development and in repair tissues and may be applicable to determining a more precise mode of action of stem cells in these processes. Isolation of perlecan from 12 to 14 week gestational age fetal knee rudiments demonstrated that perlecan in these fetal tissues was a HS-CS hybrid PG further supporting roles for CS in tissue development.

Introduction

THE CAPACITY OF MESENCHYMAL STEM CELLS (MSCs) for self-renewal and directed differentiation and their ability to modulate the local microenvironment through their anti-inflammatory and immunosuppressive properties [1–3] makes them attractive candidates for a range of cell-based therapies and considerable interest has centered around their use in regenerative medicine. MSCs are known to home to sites of injury where paracrine effector molecules and subtle extracellular matrix (ECM) feedback cues are believed to direct cell lineage development [1,4]. Demonstration of the engraftment of MSCs to defect sites can be difficult to demonstrate due to a lack of reliable specific MSC markers, yet beneficial therapeutic effects are still demonstrable for a period of weeks after administration of the MSCs, thus the precise mode of action of the MSCs in tissue repair processes remains elusive [1,4].

The aim of this study was therefore to determine whether the novel chondroitin sulfate (CS) sulfation motifs identified by monoclonal antibodies (mAbs) 4C3, 7D4, and 3B3[–] could be used to identify activated stem cell lineages involved in tissue development. The fetal human elbow was selected as a target tissue of interest since these are of a convenient size and contain a diverse number of known or putative stem cell niches in the developing articular cartilage, perichondrium,

[1]Bioimaging Unit, Cardiff School of Biosciences, University of Cardiff, United Kingdom.
[2]School of Biosciences, University of Cardiff, Cardiff, United Kingdom.
[3]Raymond Purves Laboratory, Institute of Bone and Joint Research, Kolling Institute of Medical Research, Royal North Shore Hospital and University of Sydney, St. Leonards, New South Wales, Australia.
[4]Sydney Medical School, Northern, The University of Sydney, Royal North Shore Hospital, St. Leonards, New South Wales, Australia.
[5]Graduate School of Biomedical Engineering, Faculty of Engineering, University of New South Wales, Sydney, New South Wales, Australia.

and perivascular/stromal tissues associated with the rudiment skin and hair follicle development. Earlier studies have demonstrated that the CS sulfation motifs 7D4 and 4C3 decorate cell associated proteoglycans (PGs), which serve to immobilize growth factors/morphogens actively involved in tissue development [5].

The unique distributions of these CS sulfation motifs with discrete populations of surface zone progenitor cells in knee articular cartilage [6–9] and in tissue niches associated with histogenesis and tissue differentiation [10–12] indicate that they identify an early stage of stem/progenitor cell differentiation. Previous studies indicate that these 4C3, 7D4, and 3B3[−] positive progenitor cell populations played roles in hematopoiesis, skin morphogenesis, chondrogenesis, and intervertebral disc (IVD) development [6–9,11,12]. The findings of this study indicate that these CS sulfation motifs also have important roles to play in the development of the human fetal elbow joint and its associated connective tissues.

The relevance of CS to the proposed study is also now apparent from a number of recent studies that have established roles for CS in the control of MSC proliferation and differentiation [13]. CS has an indispensable role to play in the development of MSC pluripotency [13] and oversulfated CS can induce osteogenic differentiation of human MSCs independant of bone morphogenetic protein (BMP)-2 and transforming growth factor-β1 (TGF-β1) [14]. CS can also modulate the adhesiveness of MSCs in the niche environment to ECM components such as E-cadherin and also alter integrin- dependent cell-matrix attachments influencing the development of activated MSC/progenitor cell lineages [15–19].

The elbow joint is a complex hinge joint consisting of (1) humero-radial, (2) humero-ulnar, and (3) radio-ulnar joints [20]. Numerous ligaments, tendons and muscles, and a synovial joint capsule surround the elbow joint. The articulating surfaces of the elbow joint are located between the trochlea of the humerus and ulna and between the humeral capitulum and head of the radius [20]. Ulnar and radial

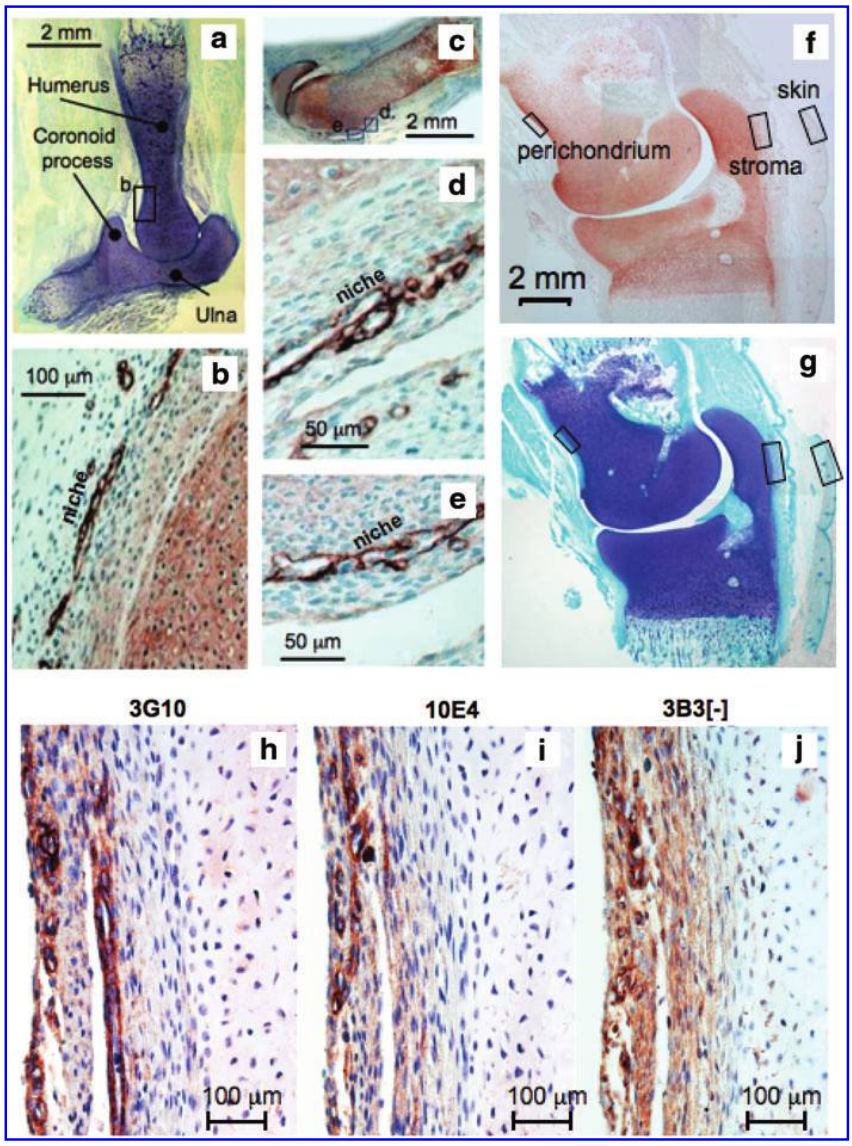

FIG. 1. Composite picture of two 12-week-old and one 14-year-old human fetal elbow joints. Toluidine blue-stained rudiments **(a, g)**. Higher power view of the *boxed area* in **(a)** depicting perlecan immunolocalization **(b)**. Macroscopic immunolocalization of perlecan in a second 12-week-old elbow joint rudiment **(c)**. The *boxed areas* **(d, e)** in segment **(c)** are also presented separately at higher magnification in **(d)** and **(e)**. Putative stem cell niches bordered by perlecan in the perichondrium **(b)** and in the surface regions of the developing articular cartilage **(d, e)** and the cartilage rudiment are labeled. Immunolocalization of perlecan **(f)** and toluidine blue-stained glycosaminoglycan **(g)** in a 14-week-old human fetal elbow. The *boxed areas* labeled skin, stroma, and perichondrium are areas of the interest, which are presented at higher magnification in later figures. Immunolocalization of Δ-HS stub epitope generated by predigestion of the section with heparitinase III and detected using mAb 3G10 **(h)**, native HS (mAb 10E4) **(i)**, and 3B3[−] CS epitope **(j)** are also depicted for the perichondrial area indicated in **(f, g)**. CS, chondroitin sulfate; HS, heparan sulfate; mAb monoclonal antibody. Color images available online at www.liebertpub.com/scd

collateral ligaments, strong fan-shaped ligaments, extend from the medial epicondyle of the humerus to the proximal ulna, and lateral epicondyle of the humerus to the head of the radius to stabilize the elbow joint preventing excessive abduction [21]. Morphological and histological studies have described the development of the human fetal elbow [21–24]; its vascular supply [25,26]; and the development of the intra-and extra-capsular ligaments of the elbow [27].

Cellular events associated with fetal diarthroidal joint formation and articular cartilage development have been extensively studied [6,28–33]. An early event in fetal joint development is the cellular condensation of mesenchyme between cartilaginous limb elements to form a joint interzone between the cartilage rudiments [23,24]. This interzone specifies the future joint line and serves as an important signaling center, containing members of the TGF-β growth and differentiation factors (GDFs) –5 & 6; BMP-2, 3 & 4 and fibroblast growth factor (FGF) –2, 4 & 13 superfamilies; BMPs and BMP-antagonists (*Chordin & Noggin*); and transcription factors that promote chondrogenesis [31,34].

The progenitor cells of the interzone give rise to the embryonic joint connective tissue, the synovial cavity and the joint articulating surfaces [6,8,9, 19,26,28]. The articular chondrocytes derive from a distinct population of GDF-5-positive interzone cells [30–33] while a Notch-1-positive progenitor cell subpopulation has also been identified within the articular cartilage surface zone [6,32,33]. Following joint cavitation, the future articular cartilage expresses a number of CS sulfation motifs identified by mAbs 3B3[–], 7D4, and 4C3 [5,7,9,11,12] on a collection of matrix and cell membrane PGs, but these appear absent from the interzone. The CS/dermatan sulphate (DS) and heparan sulfate (HS) glycosaminoglycans (GAGs), play important roles in the binding/sequestration and presentation of soluble signaling molecules in biological systems via unique sulfation sequences [5,7,9,34–38]; however, limited information is available on their specific roles in joint morphogenesis and articular cartilage development [5,9,10].

In this study, we have examined the distribution of these novel CS sulfation motifs within the fetal human elbow to better define their potential roles in its development. Discrete cell populations expressing the 7D4 and 4C3 CS sulfation motifs were identified in the perichondrium and the surface regions of the articular cartilages. The HS-substituted PG perlecan was also strongly expressed in the outermost regions of the perichondrium, hair bulbs, and stromal progenitor cell niches in close association with, but not colocalized, with the 4C3 and 7D4 CS sulfation motifs. HS-PGs such as perlecan are important constituents of stem cell niches and have roles in the establishment of growth factor and morphogen gradients in developmental tissues, which drives cellular migration and differentiation [39,40]. The role of the CS sulfation motifs in these processes, however, remains to be fully elucidated.

The perichondrium has long been known as a source of progenitor cells and a source of morphogens or signaling molecules, which direct and regulate fetal cartilage and bone formation [41–48]. With skeletal development the perichondrium becomes vascularized and in adulthood is termed the periosteum. All of the bone surfaces except those containing articular cartilage are covered by the periosteum. The periosteum/endostium are rich sources of progenitor cells, which has led to their harvest to suture over cartilage defects filled with autologous chondrocytes to promote cartilage repair. Reconstructive surgery has also utilized the periostium as a source of cells to drive cartilaginous remodeling and repair processes and support angiogenesis, osteogenesis, and chondrogenesis [45–48]. This study has further established that the CS sulfation motifs described are markers of progenitor cell populations in the inner regions of the perichondrium and in the hair bulb and rudiment-associated stromal/perivascular niches in the developmental human elbow joint.

Materials and Methods

Histochoice was an Amresco product. mAbs to perlecan domain-I (mAb A76) and IV (mAb A7L6), were obtained from abcam. Mouse monoclonals recognizing the distinct CS/DS sulfation motifs (mAbs 3B3[–], 4C3, and 7D4) have been described [11,12]. Mouse mAbs toward native HS (mAb 10E4) and

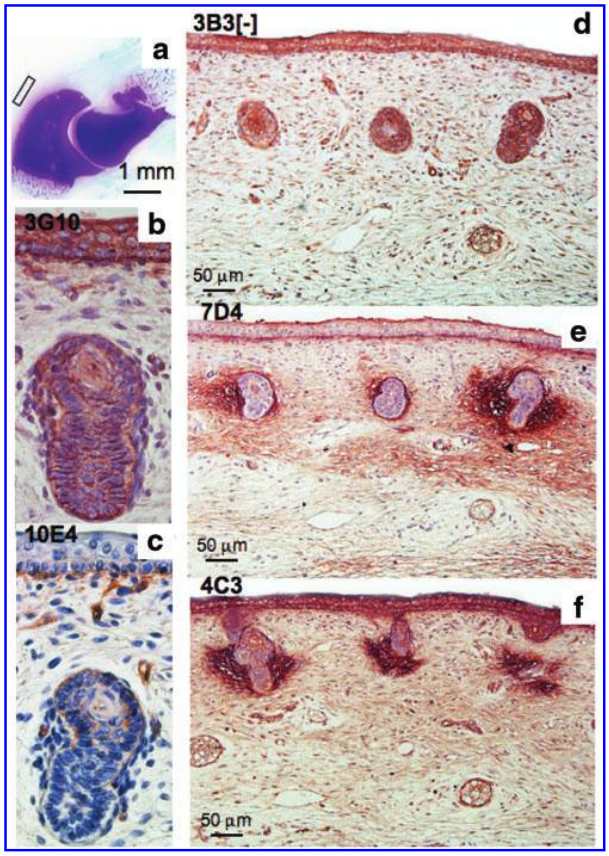

FIG. 2. Identification of Δ-HS stub epitope generated by predigestion of the section with heparitinase III and native HS immunolocalized using mAb 3G10 and 10E4 respectively in a developing hair bulb and associated with skin in a 14-week-old human fetal elbow **(a, b)**. The macroscopic toluidine blue-stained sections **(c)** the general location of the tissue area of interest. Immunolocalization of 3B3[–] CS epitope **(d)**; 7D4 CS sulfation motif **(e)** and 4C3 CS sulfation motif **(f)**. Color images available online at www.liebertpub.com/scd

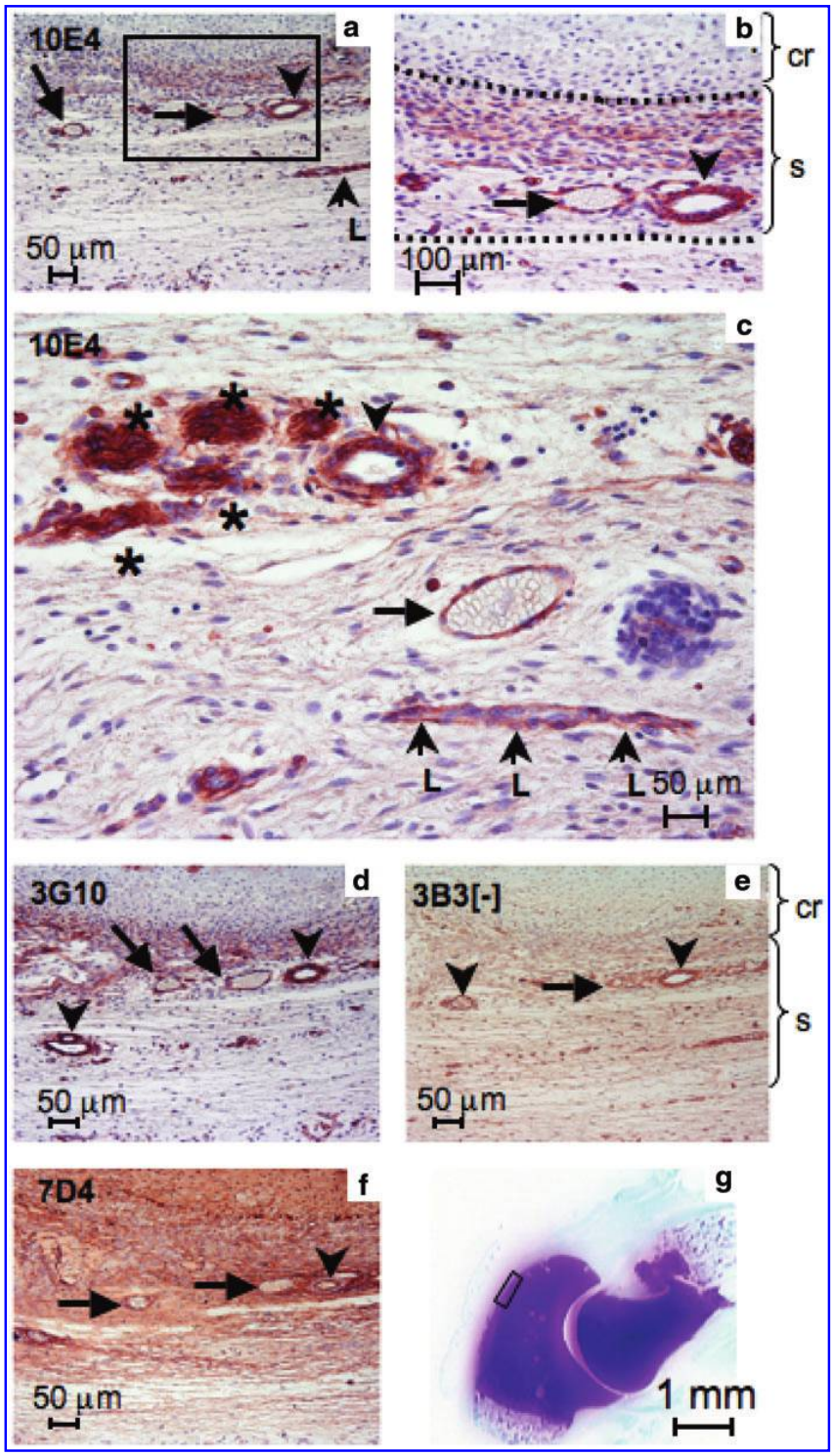

FIG. 3. Immunolocalization of native HS using mAb 10E4 **(a–c)** in a stromal niche adjacent to the ulna in a 14-week-old human fetal elbow. This is the area labeled stroma in Fig. 2a and b. The *boxed area* in **(a)** is presented at higher magnification in **(b)**. *Dotted lines* in **(b)** depict the demarcation of the cartilage rudiment (cr) and stromal tissue (s) and the edges of the loose stromal connective tissue surrounding the ulna rudiment. Δ-HS stub epitope generated by predigestion with heparitinase III is also immunolocalized in the same stromal area using mAb 3G10 **(d)** as is CS epitope 3B3[–] **(e)** and CS sulfation motif 7D4 **(f)**. The macroscopic toluidine blue-stained photo segment in **(g)** depicts the whole elbow joint with the *boxed* stromal area of interest indicated. *Arrows* depict small blood vessels containing entrapped red blood cells; *arrowhead* an arteriole; *arrow* labeled *L* denotes flattened lymphatics. The *asterisks* in **(c)** depict a 10E4 positive nerve plexus. Color images available online at www.liebertpub.com/scd

Δ-HS stubs generated by heparitinase digestion (mAb 3G10) were purchased from AMS Biotechnology. Six elbow and eight knee joints from 12 to 14-week-old human fetuses were obtained with informed consent at termination of pregnancy with ethical approval from the Human Care and Ethics Review Board of The Royal North Shore Hospital, University of Sydney.

Isolation of perlecan from human fetal knee joint rudiments

The femoral, tibial, and patellar cartilage rudiments from eight 12–14 week gestational age human fetal knees were trimmed of associated tissues, finely diced, and extracted in

6 M Urea 50 mM Tris-HCl pH 7.2 containing protease inhibitors (Roche) (5 mL) for 72 h at 4°C. The extract was separated from tissue residue by filtration through a 45 μm syringe filter and clarified by centrifugation (10,000 $g\times$ 10 min). The extract was applied to a 1 mL Q-Sepharose column and eluted with 6 M urea 50 mM Tris-HCl pH 7.2 0.3 M NaCl (buffer A, 10 mL) then with a linear gradient of 0.3–2.0 M NaCl in buffer A (20 mL). Fractions (0.25 mL) were collected into 96-well microtiter plates. Protein and sulfated GAG were measured in each fraction using the bicinchoninic acid protein assay and the metachromatic dye 1,9-dimethylmethylene blue [49]. Perlecan eluted in fractions 47–50 separated from aggrecan, which eluted in fractions 55–70. Aliquots of individual fractions were electrophoresed on 3%–8% polyacrylamide gradient (PAG) Tis-acetate gradient gels and blotted to nitrocellulose[50]. After blocking the blots were probed with antibodies to KS (mAb 5D4) and perlecan domain-I (mAb A76). Blots were also predigested with chondroitinase ABC (0.1 U/mL) in 50 mM Tris-acetate pH 6.8 containing 2% w/v bovine serum albumin then blotted with mAb 2B6(+) to the chondroitin-4-sulfate stub epitopes [50].

Some gels were also stained with toluidine blue. Samples of the perlecan pool from anion exchange chromatography were separated on 3%–8% PAG Tris-acetate gels and blotted using mAbs A76 and 2B6(+). HiMark (InVitrogen) prestained molecular weight standards were used for calibration purposes for the blotting step. Purified endothelial cell perlecan (Fig. 8A, lane 1) aggrecan from ovine articular cartilage of 2, 3, and 4-year-old sheep (Fig. 8A, lanes 2–4), CS (Fig. 8A, lane 5) and intervertebral disc (Fig. 8A, lane 6) were also run as standards.

Preparation of human fetal elbow specimens for histochemistry and immunohistochemistry

Human fetal elbows were fixed in Histochoice for 24 h. The tissues were dehydrated in graded ethanol solutions and embedded in paraplast wax. Four micrometers midsagittal microtome sections were cut and attached to SuperFrost Plus glass microscope slides (Menzel-Glaser), deparaffinized in xylene (two changes $\times$ 5 min), and rehydrated through graded ethanol washes (100%–70% v/v) to water. Sections destined for confocal immunolocalizations were cut at 7 μM and treated identically.

Histochemistry

Sections were stained for 10 min with 0.04% toluidine blue in 0.1 M sodium acetate buffer pH 4.0 to visualize tissue PGs. This was followed by 2 min counterstaining in an aqueous 1% fast-green FCF stain to differentiate areas stained for PG. Sections were also stained with hematoxylin and eosin to examine cellular morphology.

Immunoperoxidase labeling

The CS sulfation motifs 4C3, 7D4, and 3B3[−], perlecan (mAb A7L6), native HS (mAb 10E4), and Δ-HS stub epitope (mAb 3G10) were immunolocalized in 4 μm sections of human fetal elbow as specified previously [9]. The 3G10 HS stub epitope was generated by predigesting the tissue sections with heparitinase III as indicated earlier [9].

Brightfield photomicroscopy

Sections, processed as above, were digitally photographed under brightfield optics on a Leica DM6000 microscope (Leica).

Immunofluorescence and confocal laser scanning microscopy

Sections were digested in proteinase K (500 μg/mL) for 15 min at room temperature. After washing for 5 min in

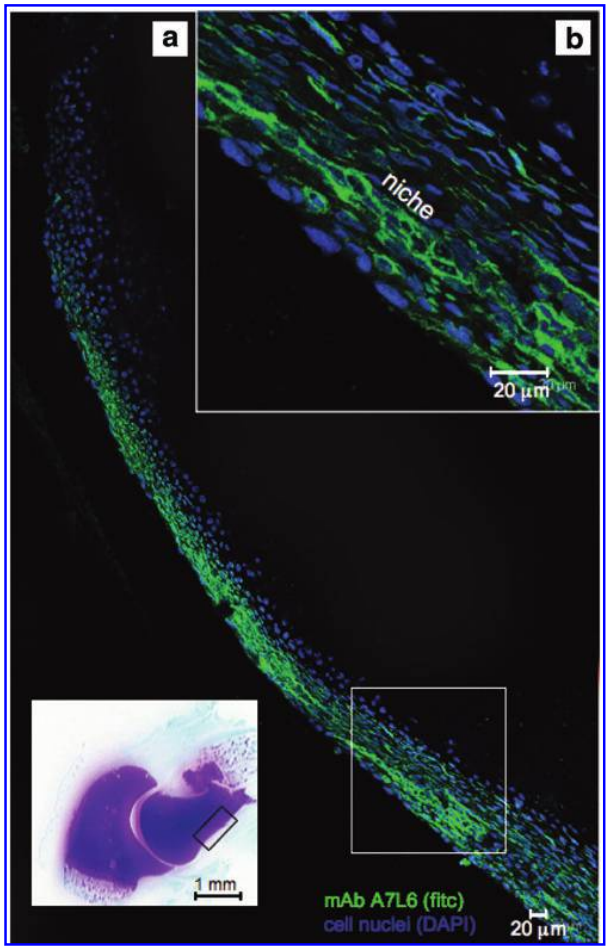

FIG. 4. Immunolocalization of perlecan in the perichondrium of a 14-week-old human fetal elbow using laser-assisted fluorescent confocal microscopy. Perlecan was immunolocalized using mAb A7L6 to perlecan domain IV and FITC-conjugated anti rat IgG, cell nuclei were stained with DAPI. The toluidine blue-stained *inset* of the fetal elbow depicts the general area of the humerus perichondrium (*boxed area*) from which the images were taken. The *boxed area* in **(a)** is also provided at higher magnification in **(b)**. Putative stem cell niches bounded by perlecan are also labeled in **(b)**. Color images available online at www.liebertpub.com/scd

phosphate-buffered saline (pH 7.4) containing 0.001% Tween-20 tissue sections were blocked with normal goat or donkey serum (1:20 dilution) for 30 min at room temperature, followed by overnight incubation at 4°C with 3B3[−], 4C3, and 7D4 hybridoma conditioned media (1:20 dilution), or mAb A7L6 (2 μg/mL), respectively. The tissue sections were then washed and a FITC-conjugated goat anti-mouse or donkey anti-rat secondary antibody (1:200 dilution) applied for 1 h at room temperature to specifically target either mouse or rat primary antibodies (ie, 3B3[−], 4C3, 7D4, and A7L6 respectively). After a final wash, sections were mounted under coverslips in Vectashield mountant (Vector Laboratories) containing either DAPI or propidium iodide for nuclear context. The fluorescently labeled tissue sections were then scanned on a Leica TCS SP2 AOBS confocal laser scanning microscope (Leica) using appropriate excitation and emission settings for DAPI (Ex max: 359 nm; Em. max: 461 nm), FITC (Ex max: 494 nm; Em max: 520 nm), and propidium iodide (Ex max 536 nm; Em max: 617 nm). Representative images were then imported into Microsoft Powerpoint worksheets to assemble the composite histology figures.

Results

Initial histological examination of two 12-week-old human fetal elbows using toluidine blue staining and immunolocalization of perlecan demonstrated the cartilaginous nature of the elbow rudiment and widespread localization of perlecan throughout the rudiments (Fig. 1a–e). Perlecan was also immunolocalized to small vessel-like structures in the perichondrial tissues (Fig. 1b, d, e). These structures did not stain with antibodies to CD31, CD34, LYVE-1, and podoplanin; thus, they did not represent vascular or lymphatic structures (data not shown). Further analysis of perlecan immunolocalization in a 14-week-old human fetal elbow also showed a widespread distribution (Fig. 1f). The surface regions of the perichondrial tissues also stained positively for native HS and Δ-HS stub epitope and the 3B3[−] CS motif (Fig. 1h–j).

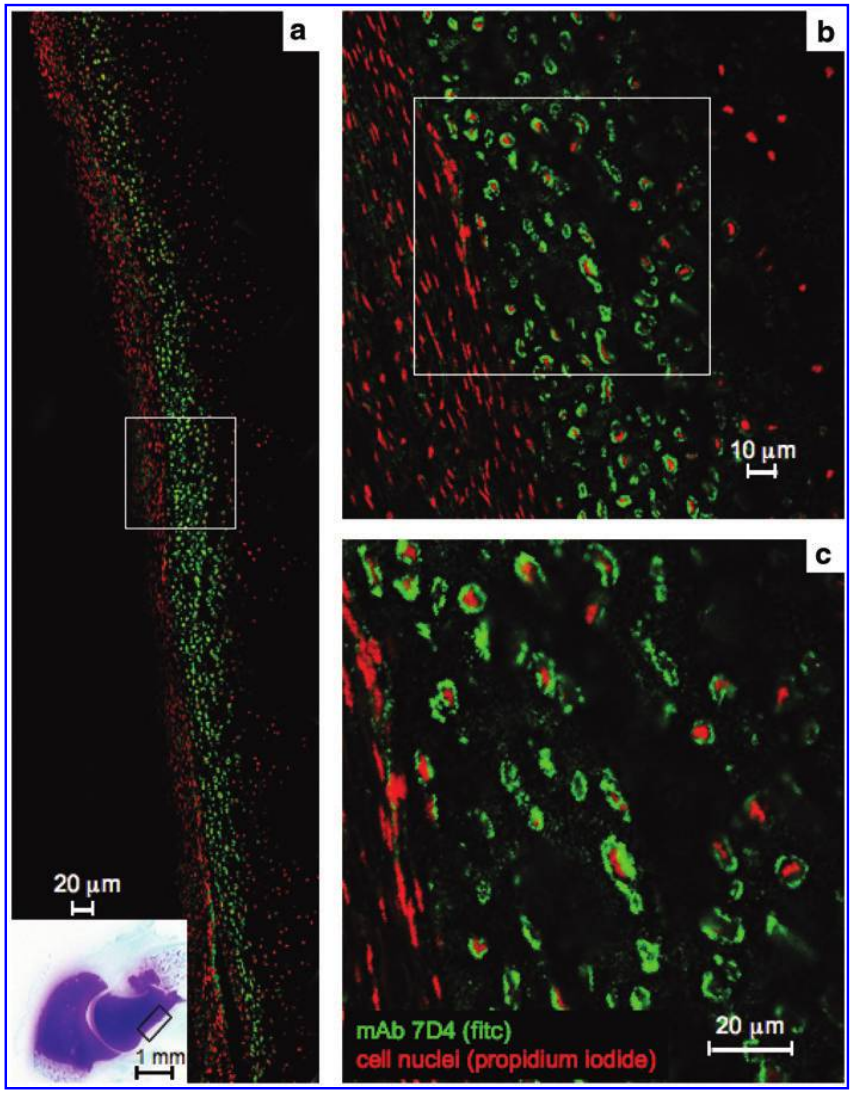

FIG. 5. Immunolocalization using fluorescent confocal microscopy of 7D4 CS sulfation motif in the humerus perichondrium of a 14-week-old human fetal elbow **(a)**. The *boxed area* in **(a)** is depicted at higher magnification in **(b)** and the *boxed area* in **(b)** at higher magnification in **(c)**. The 7D4 epitope was visualized using 7D4 mAb and FITC-conjugated anti mouse IgG, cell nuclei were stained with propidium iodide. The toluidine blue-stained macroscopic *inset* view of the elbow depicts the area of the humerus perichondrium where the confocal images were obtained. The putative perichondrial niche is labeled in **(c)** with 7D4 labeled progenitor cells, which have been released from the niche arrowed. Similar perlecan-rich niches are also evident in bright field images in Fig. 1b, d, and e. Color images available online at www.liebertpub.com/scd

The heparitinase III-generated unsaturated HS stub epitope and native HS were immunolocalized to hair bulbs and epidermis of the skin overlying the elbow (Fig. 2b). The hair had yet to erupt from the follicle but in some cases the location of the hair stem was visible in cross section within the bulb structure (Fig. 2a, b). The Δ-HS stub epitope had a more widespread distribution than native HS in the hair bulb and epidermis. Occasional small blood vessels were discernable in the dermis containing entrapped red blood cells, the endothelial cells surrounding these also expressed Δ-HS stub epitope and native HS (Fig. 2a) while native HS was localized in the basement membrane underlying the dermis (Fig. 2b). The CS sulfation motifs 3B3[−], 7D4, and 4C3 were also strongly expressed around and within the hair bulb structures (Fig. 2d–f) with the 3B3[−] CS motif associated with the hair bulb while the 7D4 and 4C3 CS sulfation motifs were associated with discrete cell populations surrounding the bulb. The 3B3[−], 7D4, and 4C3 motifs were also immunolocalized to occasional small blood vessels in the dermis and to a variable extent in the epidermis (Fig. 2d–f). The 3B3[−] motif was expressed within the hair follicle and in the epidermis, whereas the distribution of the 7D4 and 4C3 CS motifs were more extensive on the outer margins and surrounding the follicle and in the epidermis (Fig. 2d–f).

The CS sulfation motifs 3B3[−], 7D4, 4C3, Δ-HS stub epitope, and native HS were also immunolocalized to a collection of small blood vessels and arterioles in the stromal tissues adjacent to the elbow cartilage rudiments (Fig. 3a–f). Δ-HS stub epitope and native HS were both strongly immunolocalized to stromal blood vessels (Fig. 3a–d). Native HS was also immunolocalized to a nerve plexus in the stromal tissue (Fig. 3c). The 3B3[−] CS motif also had a widespread distribution in the rudiment-associated stromal tissues (Fig. 3e), whereas the 7D4 epitope was more strongly associated with the cartilage rudiment than this surrounding stromal tissue (Fig. 3f).

Confocal microscopy identified perlecan prominently in the surface regions of the perichondrium (Fig. 4a) associated with tube-like structures (Fig. 4b), these localizations were distinguishable from perlecan immunolocalized pericellularly around small blood vessels in the stromal connective tissues surrounding the elbow rudiments (Fig. 3c–f). The perichondrium contained two populations of cells of differing morphology, a more flattened surface zone population that expressed perlecan and a more rounded cell population in the inner perichondrial regions, which expressed the 7D4 and 4C3 CS epitopes. The inner perichondrial cells stained positively for the 7D4 CS sulfation motif, which appeared associated with a cell surface PG (Fig. 5a–c).

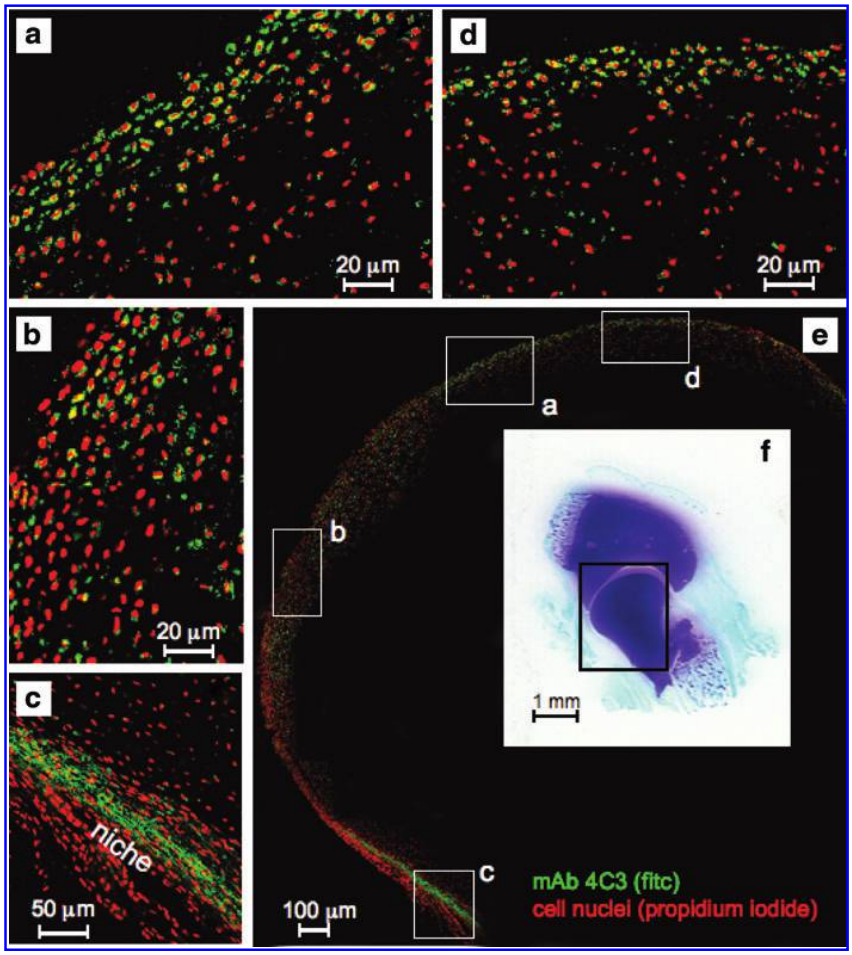

FIG. 6. Composite figure depicting the immunolocalization of 4C3 CS sulfation motif labeling activated chondroprogenitor cells in regions of the presumptive articular cartilage of the humerus and the perichondrium of a 14-week-old human fetal elbow using fluorescent confocal microscopy. The *boxed areas* **(a–d)** in photosegment **(e)** are also depicted at higher magnifications elsewhere in the figure. The 4C3 epitope was visualized using 4C3 mAb and FITC-conjugated anti mouse IgG, cell nuclei were stained with propidium iodide. The toluidine blue-stained macroscopic *inset* image depicts the area of the humerus where the confocal images were obtained. These *arrows* also depict blood vessels as indicated earlier in the legend. Color images available online at www.liebertpub.com/scd

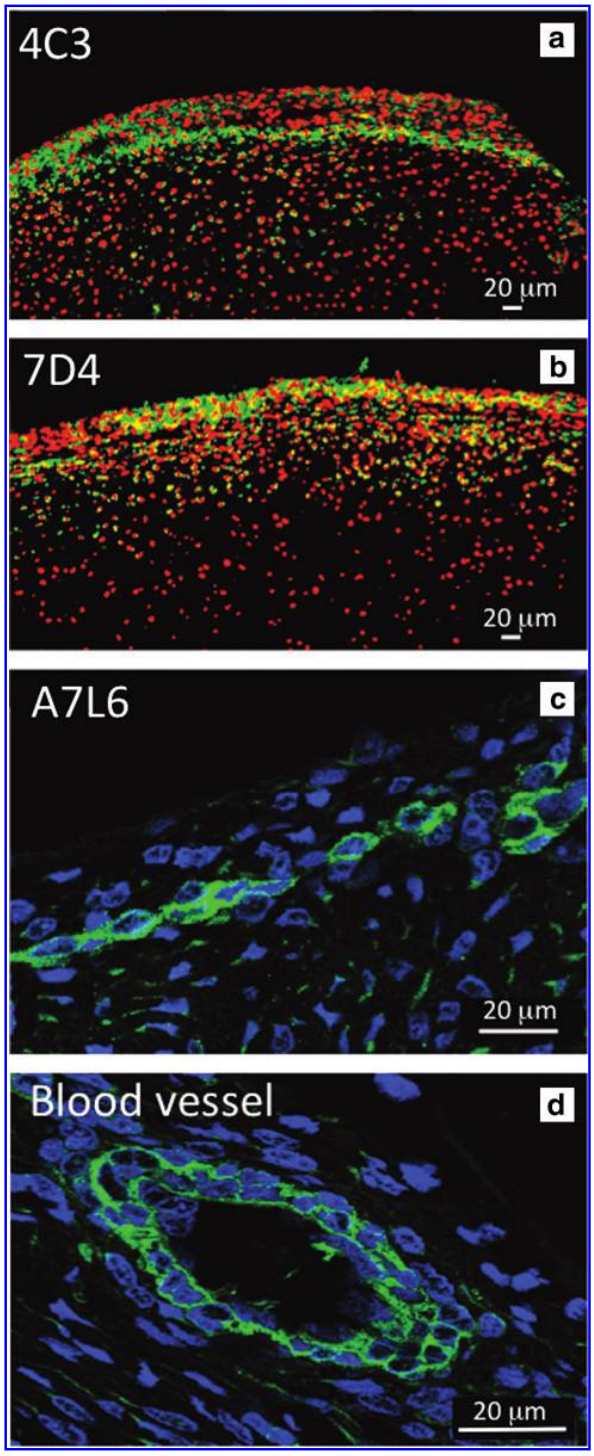

FIG. 7. Confocal immunolocalization of the 4C3 **(a)**, 7D4 **(b)**, and CS sulfation motifs in knee tibial cartilage. Perlecan displayed a similar immunolocalization of perlecan in the surface cartilage regions as in the fetal elbow **(c)**. Perlecan was also immunolocalized surrounding endothelial cells in a stromal rudiment-associated blood vessel and served as a perlecan internal positive control **(d)**. Cell nuclei are stained *red* with propidium iodide, antibody localization in *green* (FITC). Color images available online at www.liebertpub.com/scd

The 4C3 CS sulfation motif was also immunolocalized to discrete cell populations in the inner perichondrial layer (Fig. 6a) and to surface zone cells in the presumptive articular cartilage (Fig. 6b–d). The 4C3 CS sulfation motif was immunolocalized around individual cells but was not expressed by the flattened cells in the outer perichondrial layers (Fig. 6a–d). The distribution of 4C3, 7D4, and perlecan in fetal knee rudiment cartilage was similar to that found in the fetal elbow (Fig. 7a–d). Immunoblotting (Fig. 8A–D) of individual fractions from anion exchange separation of a knee rudiment extract (Fig. 8E) demonstrated successful separation of aggrecan and versican from perlecan with perlecan eluting early in the separation at ~0.4 M NaCl in the elution gradient in fractions 47–50 while aggrecan and versican eluted later in the gradient in fractions 55–70 (Fig. 8E). Further examination of the perlecan pool by immunoblotting using mAb 2B6(+) to the chondroitin-4 sulfate stubs and mAb A76 to perlecan domain-1 demonstrated a large molecular weight band of ~460 kDa in size, consistent with full-length perlecan (Fig. 8F).

Discussion

A number of publications have shown that fetal articular cartilage has a stem/progenitor cell population located within its surface regions [6,26,31,41,51] and that many of these cells express the CS sulfation motifs 4C3, 7D4, 3B3[–], and 6C3 [6,7,9]. The presence of cells expressing the 4C3 and 7D4 CS sulfation motifs within the presumptive articular cartilage and perichondrial tissue of the fetal elbow observed in this study provides further evidence of these as developmental markers. Perlecan also has a widespread distribution in articular cartilage and promotes chondrogenesis [52–56]. Perlecan was found localized to the surface regions of the perichondrium in this study where it may provide a unique niche microenvironment conducive to the maintenance of progenitor cell populations underlying the fibrous perichondrium [42,43].

The perichondrium is a layer of dense irregular connective tissue that surrounds the cartilage of developing bone. It consists of two separate layers: an outer fibrous layer and inner chondrogenic layer. The fibrous, perlecan-rich layer contains cells of a fibroblastic morphology while the chondrogenic layer contains chondroblasts or committed chondrocytes [53]. In this study these cells expressed the 4C3 and 7D4 CS epitopes, which was consistent with them as differentiation markers [5,6,11,12,57]. Our study also confirmed the findings of Malgouries et al. [58] that hair bulb cells expressed the CS sulfation motifs 4C3 and 7D4 [58], the hair bulb is a well-known stem cell niche [59,60].

We also observed CS sulfation motif expression by discrete cell populations in perivascular stromal niches adjacent to the elbow cartilage rudiments; blood vessels were also present in these stromal niches and have been suggested as a source of perivascular MSCs [61,62]. The 4C3 and 7D4 CS motifs thus had a widespread distribution in perichondrial, hair bulb, stromal/perivascular, and skin stem cell niches.

The term stem cell niche was first introduced in 1978 by Schofield [63]. The stem cell niche contains all the cellular and molecular factors in the stem cell microenvironment that interact and regulate the stem cell. The niche provides support and maintenance of the stem cell and regulation of its proliferation and may also direct downstream

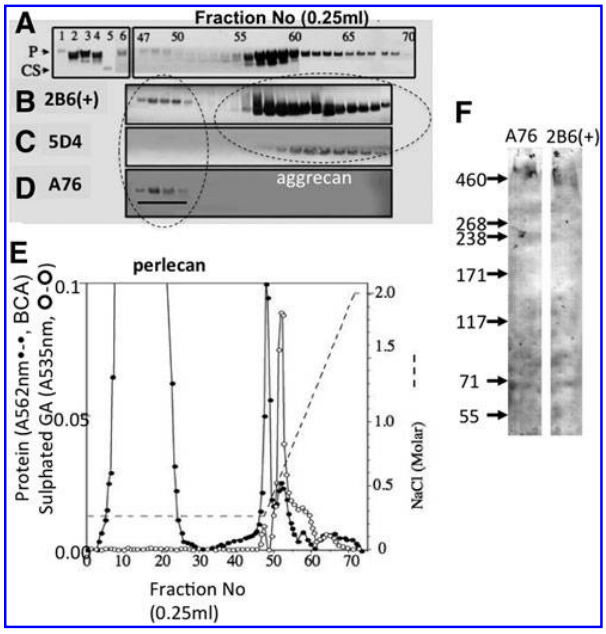

FIG. 8. Toluidine blue staining **(A)** and immunoblotting **(B–D)** of individual fractions from an anion exchange separation **(E)** demonstrating the separation of human knee rudiment perlecan from aggrecan and versican. Perlecan in fractions 47–50 was pooled and immunoblotted **(F)**. mAb 2B6(+) to the core protein chondroitin-4-sulfate stubs and mAb A76 to perlecan domain-1 identified a large molecular weight form of perlecan of ~460 kDa. This was a CS-HS hybrid proteoglycan. The *lane numbers* in **A** delineate fraction numbers from the anion exchange chromatography. The *dotted circles* depict the 2B6(+) and A76 positive perlecan bands on the blots well separated from 2B6(+) versican/aggrecan. The *dotted line* in **E** depicts the progress of the NaCL gradient elution.

differentiation and cell lineage development. Anchorage of the stem cell to ECM components or brother stem cells in the niche microenvironment is considered an important requirement for the retention of the stem cell in the niche and for its slow turnover and self-renewal in the niche. A number of interactions are important in the adhesion and retention of the stem cell in the niche [64–67]. These include interactions with the cadherin family [64], integrins, and cellular receptor-ECM (CD-44: HA) [66], gap junction formations involving the Connexin family, or niche cell-cell-stem interactions involving; Delta-1/Notch; stem cell factor-c-kit interactions. Perlecan was also an ECM component of the hair bulb, stromal/perivascular and perichondrial niches in this study. Perlecan is a component of neural and epithelial limbal stem cell niches [68,69] where the subtle variations in its HS side chain substructure and diverse repertoire of interactive ligands [70] provide a specific niche environment conducive to the regulatory conditions required for stem cell maintenance and under appropriate stimulatory conditions the activation and release of migratory progenitor cells from the niche. Stem cells and their associated niche ECMs provide specialized local microenvironments important for the retention and self-renewal of stem cells and their differentiation into multipotent cell lineages.

Perlecan is also a key component of neural [68,69], allantois [71], lymphatic [72], limbal [73], and bone marrow [74,75] stem cell niches. Perlecan modulates stem cell-ECM attachment and may modulate stem cell-integrin and stem cell-cadherin family or other cell receptor interactions such as VEGF2 [76] to influence stem cell survival, differentiation, and proliferation [70,76,77]. Extrinsic interactions with soluble growth factors such as FGF2 may also promote stem cell survival [68,69] through the Wnt signaling pathways [77]. By modulating such stem cell-matrix interactions perlecan can help retain the stem cells within the niche to undergo slow recycling and self renewal but can also influence the MSC daughter cells on the edge of the niche, which can undergo further differentiation into specific cell lineages and once freed of the adhesive constraints of the niche can migrate to distant sites driven by morphogen gradients also established by perlecan and its associated ligands.

In this study the perichondrium was a niche for progenitor cells, which subsequently migrated to populate the surface zone cartilages and participated in proliferation, differentiation, and matrix production to establish the articulating surfaces of the elbow joint. Cells of an osteoblastic lineage also reside in the perichondrium and have roles in the transformation of the femoral and tibial rudiment cartilages into bone as part of the endochondral ossification process, however, they can also participate in intramembranous bone formation.

The GAG chains of PGs are versatile tools for both storing and transferring information and much progress has been made in understanding how this contributes to cellular regulatory processes and developmental and disease processes. Until relatively recently heparin/HS and the heparanome had been the major focus in this area of developmental biology [78,79], however, a number of publications have now appeared elucidating roles for CS in tissue development [35–38,80].

Ongoing studies will undoubtedly identify specific CS sequences and charge localizations and their interactive ligands and how they participate in the biological processes that shape tissue development and repair. The CS sulfation motifs 7D4 and 4C3 on cell-associated PGs serve to immobilize growth factors/morphogens actively involved in tissue development [5,11,12,57]. The unique distributions of these CS sulfation motifs with surface zone progenitor cells in articular cartilage [6–9] and in tissue niches associated with histogenesis and tissue differentiation [10–12] suggests that they may identify an early stage of stem/progenitor cell differentiation. Previous studies indicate that these progenitor cell populations play roles in hematopoiesis, skin morphogenesis, chondrogenesis, and IVD development [6–9,11,12].

The findings of this study indicate they also have important roles to play in the development of the human fetal elbow joint and associated connective tissues. Moreover, detection of the 4C3 and 7D4 positive progenitor cells may provide a means of monitoring their roles in joint development. The precise mode of action of MSCs/progenitor cells in tissue repair and development has been hampered by the lack of definitive markers to identify these cells, the 4C3 and 7D4 CS sulfation motifs are expressed by activated migratory stem cell populations in developing/remodeling tissues and thus may represent a useful means of monitoring

such cells. Perlecan was subsequently isolated in this study from human fetal knee joint rudiments using anion exchange chromatography. Immunoblotting demonstrated that perlecan in fetal rudiment cartilage was a hybrid CS-HS PG.

Conclusions

The application of mAbs to the CS sulfation motifs 4C3, 7D4, and 3B3[−] to localize and differentiate the activated progenitor cell populations from the resident connective tissue cell populations may be useful in their identification and elucidation of their prospective roles in tissue development and ECM remodeling.

Acknowledgment

Funded by NHMRC project grant 352562 and 1004032.

Author Disclosure Statement

No competing financial interests exist.

References

1. Caplan AI. (2009). Why are MSCs therapeutic? New data: new insight. J Pathol 217:318–324.
2. Caplan AI. (2008). All MSCs are pericytes? Cell Stem Cell 3:229–230.
3. Caplan AI. (2009). New era of cell-based orthopedic therapies. Tissue Eng Part B Rev 15:195–200.
4. Dimarino AM, AI Caplan and TL Bonfield. (2013). Mesenchymal stem cells in tissue repair. Front Immunol 4:201.
5. Caterson B. (2012). Fell-Muir Lecture: chondroitin sulphate glycosaminoglycans: fun for some and confusion for others. Int J Exp Pathol 93:1–10.
6. Dowthwaite GP, JC Bishop, SN Redman, IM Khan, P Rooney, DJ Evans, L Haughton, Z Bayram, S Boyer, et al. (2004). The surface of articular cartilage contains a progenitor cell population. J Cell Sci 117:889–897.
7. Hayes AJ, D Tudor, MA Nowell, B Caterson and CE Hughes. (2008). Chondroitin sulfate sulfation motifs as putative biomarkers for isolation of articular cartilage progenitor cells. J Histochem Cytochem 56:125–138.
8. Hollander AP, SC Dickinson and W Kafienah. (2010). Stem cells and cartilage development: complexities of a simple tissue. Stem Cells 28:1992–1996.
9. Melrose J, MD Isaacs, SM Smith, CE Hughes, CB Little, B Caterson and AJ Hayes. (2012). Chondroitin sulphate and heparan sulphate sulphation motifs and their proteoglycans are involved in articular cartilage formation during human foetal knee joint development. Histochem Cell Biol 138:461–475.
10. Hayes AJ, CE Hughes, JR Ralphs and B Caterson. (2011). Chondroitin sulphate sulphation motif expression in the ontogeny of the intervertebral disc. Eur Cell Mater 221:1–14.
11. Sorrell JM, AM Lintala, F Mahmoodian and B Caterson. (1988). Epitope-specific changes in chondroitin sulfate/dermatan sulfate proteoglycans as markers in the lymphopoietic and granulopoietic compartments of developing bursae of Fabricius. J Immunol 140:4263–4270.
12. Sorrell JM, F Mahmoodian, IA Schafer, B Davis and B Caterson. (1990). Identification of monoclonal antibodies that recognize novel epitopes in native chondroitin/dermatan sulfate glycosaminoglycan chains: their use in mapping functionally distinct domains of human skin. J Histochem Cytochem 38:393–402.
13. Izumikawa T, B Sato and H Kitagawa. (2014). Chondroitin sulfate is indispensable for pluripotency and differentiation of mouse embryonic stem cells. Sci Rep 4:3701.
14. Buttner M, S Moller, M Keller, D Huster, J Schiller, M Schnabelrauch, P Dieter and U Hempel. (2013). Oversulfated chondroitin sulfate derivatives induce osteogenic differentiation of hMSC independent of BMP-2 and TGF-beta1 signalling. J Cell Physiol 228:330–340.
15. You J, Y Zhang, Z Li, Z Lou, L Jin and X Lin. (2014). Drosophila perlecan regulates intestinal stem cell activity via cell-matrix attachment. Stem Cell Reports 2:761–769.
16. Gao H, X Wu and N Fossett. (2013). Drosophila E-cadherin functions in hematopoietic progenitors to maintain multipotency and block differentiation. PLoS One 8:e74684.
17. Klingener M, M Chavali, J Singh, N McMillan, A Coomes, PJ Dempsey, EI Chen and A Aguirre. (2014). N-cadherin promotes recruitment and migration of neural progenitor cells from the SVZ neural stem cell niche into demyelinated lesions. J Neurosci 34:9590–9606.
18. Schueller-Weidekamm C and F Kainberger. (2008). [The elbow joint—a diagnostic challenge: anatomy, biomechanics, and pathology]. Radiologe 48:1173–1185.
19. Edwards JC, LS Wilkinson, HM Jones, P Soothill, KJ Henderson, KJ Worral and AA Pitsillides. (1994). The formation of human synovial joint cavities: a possible role for hyaluronan and CD44 in altered interzone cohesion. J Anat 185:355–367.
20. Mahasen LM and SA Sadek. (2000). Developmental morphological and histological studies on structures of the human fetal elbow joint. Cells Tissues Organs 166:359–372.
21. Merida-Velasco JA, I Sanchez-Montesinos, H Espin-Ferra, JR Merida-Velasco, JF Rodriguez-Vazquez and J Jimenez-Collado. (2000). Development of the human elbow joint. Anat Rec 258:166–175.
22. Gray DJ and E Gardner. (1951). Prenatal development of the human elbow joint. Am J Anat 88:429–469.
23. Reidenbach MM and HM Schmidt. (1994). Vascularization of the fetal elbow joint. Ann Anat 176:303–310.
24. Reidenbach MM and HM Schmidt. (1994). Cartilage canals in the fetal elbow joint in man. Acta Anat (Basel) 149:195–202.
25. Patten B. (1981). *Foundation of Embryology.* McGraw-Hill, New York.
26. Archer CW, GP Dowthwaite and P Francis-West. (2003). Development of synovial joints. Birth Defects Res C Embryo Today 69:144–155.
27. Pacifici M, E Koyama and M Iwamoto. (2005). Mechanisms of synovial joint and articular cartilage formation: recent advances, but many lingering mysteries. Birth Defects Res C Embryo Today 75:237–248.
28. Pacifici M, E Koyama, Y Shibukawa, C Wu, Y Tamamura, M Enomoto-Iwamoto and M Iwamoto. (2006). Cellular and molecular mechanisms of synovial joint and articular cartilage formation. Ann N Y Acad Sci 1068:74–86.
29. Gardner E and R O'Rahilly. (1968). The early development of the knee joint in staged human embryos. J Anat 102: 289–299.
30. Francis-West PH, A Abdelfattah, P Chen, C Allen, J Parish, R Ladher, S Allen, S MacPherson, FP Luyten and CW Archer. (1999). Mechanisms of GDF-5 action during skeletal development. Development 126:1305–1315.
31. Koyama E, Y Shibukawa, M Nagayama, H Sugito, B Young, T Yuasa, T Okabe, T Ochiai, N Kamiya, et al.

(2008). A distinct cohort of progenitor cells participates in synovial joint and articular cartilage formation during mouse limb skeletogenesis. Dev Biol 316:62–73.
32. Hayes AJ, GP Dowthwaite, SV Webster and CW Archer. (2003). The distribution of Notch receptors and their ligands during articular cartilage development. J Anat 202: 495–502.
33. Williams R, L Nelson, GP Dowthwaite, DJ Evans and CW Archer. (2009). Notch receptor and Notch ligand expression in developing avian cartilage. J Anat 215:159–169.
34. Cortes M, AT Baria and NB Schwartz. (2009). Sulfation of chondroitin sulfate proteoglycans is necessary for proper Indian hedgehog signaling in the developing growth plate. Development 136:1697–1706.
35. Hitchcock AM, KE Yates, CE Costello and J Zaia. (2008). Comparative glycomics of connective tissue glycosaminoglycans. Proteomics 8:1384–1397.
36. Kondo A, W Li, T Nakagawa, M Nakano, N Koyama, X Wang, J Gu, E Miyoshi and N Taniguchi. (2006). From glycomics to functional glycomics of sugar chains: identification of target proteins with functional changes using gene targeting mice and knock down cells of FUT8 as examples. Biochim Biophys Acta1764:1881–1889.
37. Ly M, TN Laremore and RJ Linhardt. (2010). Proteoglycomics: recent progress and future challenges. OMICS 14: 389–399.
38. Nandini CD and K Sugahara. (2006). Role of the sulfation pattern of chondroitin sulfate in its biological activities and in the binding of growth factors. Adv Pharmacol 53:253–279.
39. Princivalle M and A de Agostini. (2002). Developmental roles of heparan sulfate proteoglycans: a comparative review in Drosophila, mouse and human. Int J Dev Biol 46: 267–278.
40. Yan D and X Lin. (2009). Shaping morphogen gradients by proteoglycans. Cold Spring Harb Perspect Biol 1:a002493.
41. Arai F, O Ohneda, T Miyamoto, XQ Zhang and T Suda. (2002). Mesenchymal stem cells in perichondrium express activated leukocyte cell adhesion molecule and participate in bone marrow formation. J Exp Med 195: 1549–1563.
42. Bleys RL, M Popko, JW De Groot and EH Huizing. (2007). Histological structure of the nasal cartilages and their perichondrial envelope. II. The perichondrial envelope of the septal and lobular cartilage. Rhinology 45:153–157.
43. Colnot C, C Lu, D Hu and JA Helms. (2004). Distinguishing the contributions of the perichondrium, cartilage, and vascular endothelium to skeletal development. Dev Biol 269:55–69.
44. Kronenberg HM. (2007). The role of the perichondrium in fetal bone development. Ann NY Acad Sci 1116:59–64.
45. Boccieri A and TM Marianetti. (2010). Perichondrium graft: harvesting and indications in nasal surgery. J Craniofac Surg 21:40–44.
46. Bouwmeester PS, R Kuijer, GN Homminga, SK Bulstra and RG Geesink. (2002). A retrospective analysis of two independent prospective cartilage repair studies: autogenous perichondrial grafting versus subchondral drilling 10 years post-surgery. J Orthop Res 20:267–273.
47. Karacalar A, A Korkmaz and N Icten. (2005). A perichondrial flap for functional purposes in rhinoplasty. Aesthetic Plast Surg 29:256–260.
48. Ulutas K, A Menderes, C Karaca and S Ozkal. (2005). Repair of cartilage defects with periosteal grafts. Br J Plast Surg 58:65–72.
49. Melrose J, ES Fuller, PJ Roughley, MM Smith, B Kerr, CE Hughes, B Caterson and CB Little. (2008). Fragmentation of decorin, biglycan, lumican and keratocan is elevated in degenerate human meniscus, knee and hip articular cartilages compared with age-matched macroscopically normal and control tissues. Arthritis Res Ther 10:R79.
50. Melrose J, P Ghosh and TK Taylor. (2001). A comparative analysis of the differential spatial and temporal distributions of the large (aggrecan, versican) and small (decorin, biglycan, fibromodulin) proteoglycans of the intervertebral disc. J Anat 198:3–15.
51. Alsalameh S, R Amin, T Gemba and M Lotz. (2004). Identification of mesenchymal progenitor cells in normal and osteoarthritic human articular cartilage. Arthritis Rheum 50:1522–1532.
52. Melrose J, P Roughley, S Knox, S Smith, M Lord and JM Whitelock. (2006). The structure, location, and function of perlecan, a prominent pericellular proteoglycan of fetal, postnatal, and mature hyaline cartilages. J Biol Chem 281: 36905–36914.
53. Melrose J, S Smith, M Cake, R Read and J Whitelock. (2005). Perlecan displays variable spatial and temporal immunolocalisation patterns in the articular and growth plate cartilages of the ovine stifle joint. Histochem Cell Biol 123:561–571.
54. Melrose J, S Smith and J Whitelock. (2004). Perlecan immunolocalises to perichondral vessels and canals in human foetal cartilagenous promordia in early vascular and matrix remodelling events associated with diarthrodial-joint development. J Histochem Cytochem 52:1405–1413.
55. Smith SM, C Shu and J Melrose. (2010). Comparative immunolocalisation of perlecan with collagen II and aggrecan in human foetal, newborn and adult ovine joint tissues demonstrates perlecan as an early developmental chondrogenic marker. Histochem Cell Biol 134:251–263.
56. Gomes RR, Jr., MC Farach-Carson and DD Carson. (2004). Perlecan functions in chondrogenesis: insights from in vitro and in vivo models. Cells Tissues Organs 176:79–86.
57. Caterson B, F Mahmoodian, JM Sorrell, TE Hardingham, MT Bayliss, SL Carney, A Ratcliffe and H Muir. (1990). Modulation of native chondroitin sulphate structure in tissue development and in disease. J Cell Sci 97:411–417.
58. Malgouries S, S Thibaut and BA Bernard. (2008). Proteoglycan expression patterns in human hair follicle. Br J Dermatol 158:234–242.
59. Fantauzzo KA and AM Christiano. (2011). There and back again: hair follicle stem cell dynamics. Cell Stem Cell 8:8–9.
60. Hsu YC, HA Pasolli and E Fuchs. (2011). Dynamics between stem cells, niche, and progeny in the hair follicle. Cell 144:92–105.
61. da Silva Meirelles L, AI Caplan and NB Nardi. (2008). In search of the in vivo identity of mesenchymal stem cells. Stem Cells 26:2287–2299.
62. Crisan M, S Yap, L Casteilla, CW Chen, M Corselli, TS Park, G Adriolo, B Sun, B Zheng, et al. (2008). A perivascular origin for mesenchymal stem cells in multiple human organs. Cell Stem Cell 3:301–313.
63. Schofield R. (1978). The relationship between the spleen colony-forming cell and the haemopoietic stem cell. Blood Cells 4:7–25.
64. Malaguti M, PA Nistor, G Blin, A Pegg, X Zhou and S Lowell. (2013). Bone morphogenic protein signalling suppresses differentiation of pluripotent cells by maintaining expression of E-Cadherin. Elife 2:e01197.

65. Marthiens V, I Kazanis, L Moss, K Long and C Ffrench-Constant. (2010). Adhesion molecules in the stem cell niche—more than just staying in shape? J Cell Sci 123:1613–1622.
66. Qu C, K Rilla, R Tammi, M Tammi, H Kroger and MJ Lammi. (2014). Extensive CD44-dependent hyaluronan coats on human bone marrow-derived mesenchymal stem cells produced by hyaluronan synthases HAS1, HAS2 and HAS3. Int J Biochem Cell Biol 48:45–54.
67. Chen S, M Lewallen and T Xie. (2013). Adhesion in the stem cell niche: biological roles and regulation. Development 140:255–265.
68. Kerever A, J Schnack, D Vellinga, N Ichikawa, C Moon, E Arikawa-Hirsaswa, JT Efird and F Mercier. (2007). Novel extracellular matrix structures in the neural stem cell niche capture the neurogenic factor fibroblast growth factor 2 from the extracellular milieu. Stem Cells 25:2146–2157.
69. Kerever A, F Mercier, R Nonaka, S de Vega, Y Oda, B Zalc, Y Okada, N Hattori, Y Yamada and E Arikawa-Hirasawa. (2014). Perlecan is required for FGF-2 signaling in the neural stem cell niche. Stem Cell Res 12:492–505.
70. Whitelock JM, J Melrose and RV Iozzo. (2008). Diverse cell signaling events modulated by perlecan. Biochemistry 47:11174–11183.
71. Mikedis MM and KM Downs. (2009). Collagen type IV and Perlecan exhibit dynamic localization in the Allantoic Core Domain, a putative stem cell niche in the murine allantois. Dev Dyn 238:3193–3204.
72. Grigorian M, T Liu, U Banerjee and V Hartenstein. (2013). The proteoglycan Trol controls the architecture of the extracellular matrix and balances proliferation and differentiation of blood progenitors in the Drosophila lymph gland. Dev Biol 384:301–312.
73. Schlotzer-Schrehardt U, T Dietrich, K Saito, L Sorokin, T Sasaki, M Paulsson and FE Kruse. (2007). Characterization of extracellular matrix components in the limbal epithelial stem cell compartment. Exp Eye Res 85:845–860.
74. Chen XD, V Dusevich, JQ Feng, SC Manolaga and RL Jilka. (2007). Extracellular matrix made by bone marrow cells facilitates expansion of marrow-derived mesenchymal progenitor cells and prevents their differentiation into osteoblasts. J Bone Miner Res 22:1943–1956.
75. Schofield KP, JT Gallagher and G David. (1999). Expression of proteoglycan core proteins in human bone marrow stroma. J Biochem 343 Pt 3:663–668.
76. Lord MS, CY Chuang, J Melrose, MJ Davies, RV Iozzo and JM Whitelock. (2014). The role of vascular-derived perlecan in modulating cell adhesion, proliferation and growth factor signaling. Matrix Biol 35:112–122.
77. Kamimura K, K Ueno, J Nakagawa, R Hamada, M Saitoe and N Maeda. (2013). Perlecan regulates bidirectional Wnt signaling at the Drosophila neuromuscular junction. J Cell Biol 200:219–233.
78. Ori A, MC Wilkinson and DG Fernig. (2011). A systems biology approach for the investigation of the heparin/heparan sulfate interactome. J Biol Chem 286:19892–19904.
79. Turnbull JE, RL Miller, Y Ahmed, TM Puvirajesinghe and SE Guimond. (2010). Glycomics profiling of heparan sulfate structure and activity. Methods Enzymol 480:65–85.
80. Sugahara K, T Mikami, T Uyama, S Mizuguchi, K Nomura and H Kitagawa. (2003). Recent advances in the structural biology of chondroitin sulfate and dermatan sulfate. Curr Opin Struct Biol 13:612–620.

Address correspondence to:
Dr. James Melrose
Raymond Purves Laboratory
Institute of Bone and Joint Research
Kolling Institute of Medical Research
Level 10, B6
St. Leonards 2065
New South Wales
Australia

E-mail: james.melrose@sydney.edu.au

Received for publication February 27, 2016
Accepted after revision April 11, 2016
Prepublished on Liebert Instant Online XXXX XX, XXXX